

# Vibrational properties of the Si(111)Ga( $\sqrt{3} \times \sqrt{3}$ ) surface

J. Schmidt and H. Ibach

*Institut für Grenzflächenforschung und Vakuumphysik, Forschungszentrum Jülich, D-52425 Jülich, Germany*

J. E. Müller

*Institut für Schicht- und Ionentechnik, Forschungszentrum Jülich, D-52425 Jülich, Germany*

(Received 4 August 1994)

The adatom-substrate interaction on the Si(111)Ga( $\sqrt{3} \times \sqrt{3}$ )R30° structure was studied with high-resolution electron-energy-loss spectroscopy and *ab initio* total-energy cluster calculations. Energy losses at 100, 200, 340, 480, and 550 cm<sup>-1</sup> were identified as the folded-back part of the Rayleigh wave, the Ga adatom vibration, a breathing mode of a GaSi<sub>4</sub> cluster, and two different Si-Si stretching vibrations, respectively. The dispersion of these modes, measured along the  $\bar{\Gamma}\bar{K}$  direction of the (1×1) surface Brillouin zone, was found to be weak.

## I. INTRODUCTION

A ( $\sqrt{3} \times \sqrt{3}$ )R30° reconstruction is induced on the Si(111) surface by a number of different metals.<sup>1</sup> It consists of a 1/3 monolayer (ML) of metal adatoms that occupy half of the threefold  $T_4$  sites. Each adatom is located directly above a Si atom of the second layer, and is bonded to three Si surface atoms, such that all surface dangling bonds are saturated. A structural model of the reconstructed surface in real and momentum space is shown in Fig. 1. The general features of this model have been confirmed by previous experimental and theoretical work<sup>2-5</sup> and are now well established. However, the Ga/Si(111) system has received renewed interest after Martinez *et al.* reported giant adatom vibrations at

800 K.<sup>6</sup> These authors measured the vertical positions of the Ga atoms relative to the underlying Si layers using the x-ray standing wave method, and found that the distribution of Ga heights increased anomalously with temperature. Martinez *et al.* attributed the anomalous broadening of their data to large vibrational amplitudes of the adatoms, and predicted a pronounced decrease of the corresponding frequency with increasing temperature. For room temperature the predicted vibration frequency was ca. 100 cm<sup>-1</sup>. These considerations were partially based on a vibrational study of the Ga/Si(111) system with inelastic He scattering by Doak,<sup>7</sup> in which a dispersionless optical mode at about 100 cm<sup>-1</sup> was observed. Doak assigned this mode to either a vibration of the Ga adatom or a vibration of a cluster of atoms including the adsorbate atom. Since no higher-lying modes were found in the experiment of Doak, Martinez *et al.* assumed that the 100 cm<sup>-1</sup> mode was due to the adatom vibration.

In the present work we present and interpret the vibrational spectrum of the Si(111)Ga ( $\sqrt{3} \times \sqrt{3}$ )R30° system which was measured by high-resolution electron-energy-loss spectroscopy (HREELS). In addition to the 100 cm<sup>-1</sup> vibration, we found vibrational modes at 200, 340, 480, and 550 cm<sup>-1</sup>. With the help of *ab initio* calculations and by comparison with previous work, we conclude that the Ga vibration corresponds to the energy loss at 200 cm<sup>-1</sup>. We also demonstrate that the potential energy variation along the normal coordinate of the 200 cm<sup>-1</sup> Ga vibration shows no indication of a softening that could lead to large vibrational amplitudes at high temperatures. On the other hand, the 100 cm<sup>-1</sup> vibration, which does exhibit large vibrational amplitudes at 800 K, involves displacements of the surface Si atoms as well as of the Ga adatoms.

## II. EXPERIMENTS

The experiments were carried out in a two-level stainless steel ultrahigh-vacuum chamber. The lower level

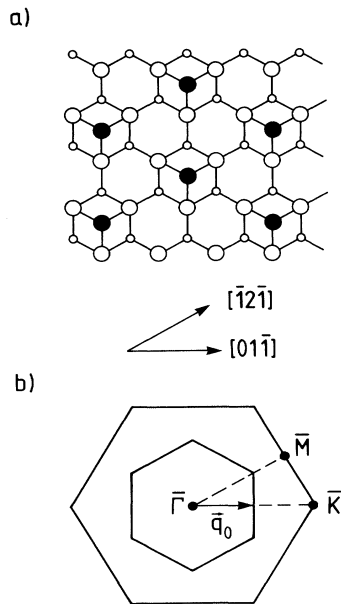


FIG. 1. (a) Structural model of the Si(111)Ga( $\sqrt{3} \times \sqrt{3}$ )R30° structure; (b) the corresponding surface Brillouin zone inscribed into the Si(111)(1×1) surface Brillouin zone.

housed the high-resolution electron-energy-loss spectrometer, while the upper level contained a cylindrical mirror analyzer for Auger electron spectroscopy, a three-grid low-energy electron-diffraction (LEED) optics, and a quadrupole mass spectrometer for residual gas analysis. The vacuum in the chamber was produced by a turbomolecular pump, an ion getter pump, and a liquid nitrogen cooled titanium sublimation pump. After baking out the chamber, a base pressure of about  $5 \times 10^{-11}$  mbar was achieved, the residual gas being mostly hydrogen. The samples, of about  $14 \times 14$  mm<sup>2</sup> in size, were cut from a Si(111) *n*-type wafer with  $\rho = 30\text{--}60$   $\Omega$  cm, and were placed in a vacuum without any *ex situ* cleaning. Annealing at 850 °C to desorb the native oxide was sufficient to produce a sharp  $(7 \times 7)$  LEED pattern. The preparation of the  $\text{Ga}(\sqrt{3} \times \sqrt{3})R30^\circ$  surface followed the recipes known from the literature.<sup>3,8</sup> The samples (held at room temperature) were exposed to a Ga beam from a precleaned and outgassed effusion cell operating at 1100 °C. The deposition rate was approximately 0.1 ML per minute as estimated with a quartz microbalance. After deposition of about 1/3 ML of Ga and annealing the sample at 500 °C a clear  $(\sqrt{3} \times \sqrt{3})$  LEED pattern was observed. Heating was performed by electron bombardment of the back side of the crystal. The sample could be cooled with liquid He. However, spectra recorded at 40 K showed no significant change compared to those recorded at room temperature. The temperature was measured with a NiCr-Ni thermocouple attached to the sample holder.

Figure 2(a) shows an EELS spectrum of the  $\text{Si}(111)\text{Ga}(\sqrt{3} \times \sqrt{3})R30^\circ$  surface recorded in the specular direction, corresponding to the  $\bar{\Gamma}$  point of the surface Brillouin zone (SBZ). The energy of the incident beam was  $E_0 = 6.5$  eV, and the elastic peak had a full width at half maximum of  $30$   $\text{cm}^{-1}$ . The spectrum shows distinct losses at 200, 340, 480, and  $550$   $\text{cm}^{-1}$ , as well as a small loss at about  $100$   $\text{cm}^{-1}$ , which can be seen as a shoulder on the energy-loss side of the elastic peak. The broad structure at  $800\text{--}1000$   $\text{cm}^{-1}$  can be ascribed to silicon carbide,<sup>9</sup> which is formed by high-temperature decomposition of CH groups in the course of the preparation of the  $(7 \times 7)$  structure. Si-C vibrations are known to have a strong dynamic dipole moment, so that even small amounts of silicon carbide give rise to distinct peaks in EELS spectra. The estimated carbon coverage on the surface was less than 0.01.

Figure 2(b) shows an off-specular spectrum recorded with  $E_0 = 15$  eV and a momentum transfer of  $q_{\parallel} = 0.2q_0$ , where  $q_0$  is the wave vector from the center of the  $(\sqrt{3} \times \sqrt{3})$  SBZ to the zone boundary in the  $[01\bar{1}]$  direction [the  $\bar{\Gamma}\bar{K}$  direction of the  $\text{Si}(111)(1 \times 1)$  SBZ; see Fig. 1(b)]. The peak at  $\sim 100$   $\text{cm}^{-1}$  is now clearly resolved. Note the appearance of the corresponding energy-gain peak on the left side of the elastic peak. The  $340$   $\text{cm}^{-1}$  loss can be clearly recognized, while the peak found at  $480$   $\text{cm}^{-1}$  at  $\bar{\Gamma}$  is shifted to about  $450$   $\text{cm}^{-1}$ . The losses at  $200$  and  $550$   $\text{cm}^{-1}$  are not observable with the scattering conditions used for this spectrum.

Figure 3 shows the dispersion of the observed surface modes throughout the whole  $(\sqrt{3} \times \sqrt{3})$  SBZ along the

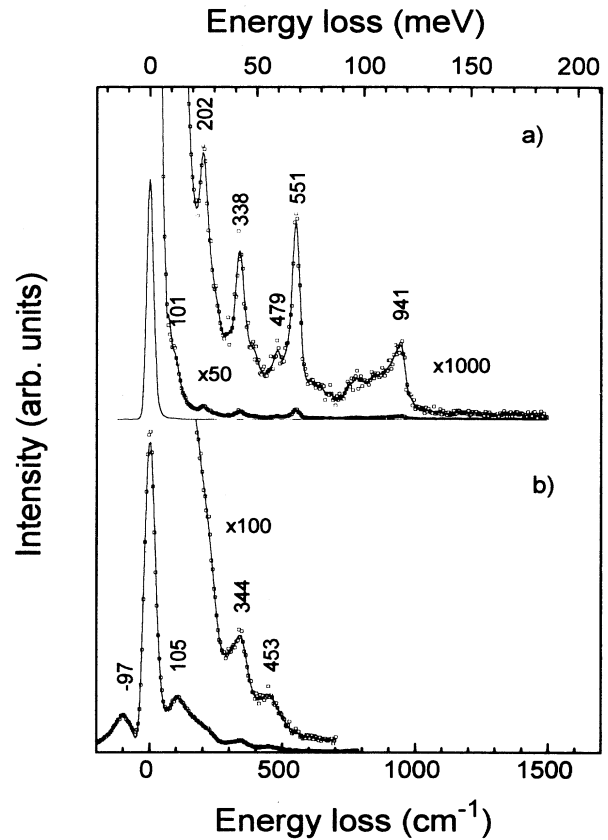


FIG. 2. Electron-energy-loss spectra of the  $\text{Si}(111)\text{Ga}(\sqrt{3} \times \sqrt{3})R30^\circ$  surface for (a)  $q_{\parallel} = 0$ , and (b)  $q_{\parallel} = 0.2q_0$ .

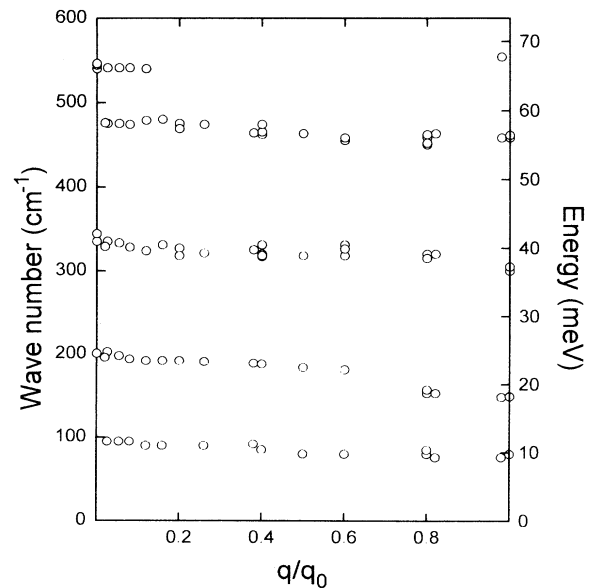


FIG. 3. Surface phonon dispersion of the  $\text{Si}(111)\text{Ga}(\sqrt{3} \times \sqrt{3})R30^\circ$  surface along  $\bar{\Gamma}\bar{K}$ .

Si[011] direction. Off-specular spectra were recorded at different primary energies in the range from 6.5 to 55 eV, and only well resolved peaks similar in quality to those shown in Fig. 2(b) were included in the dispersion curves. It is apparent that the measured modes show little dispersion throughout the SBZ.

The  $100\text{ cm}^{-1}$  mode was already reported by Doak in a vibrational study of the Si(111)Ga( $\sqrt{3}\times\sqrt{3}$ ) $R30^\circ$  surface using helium scattering. Doak also observed an acoustic mode with a zone boundary frequency of  $80\text{ cm}^{-1}$ .<sup>7</sup> We have not been able to observe the acoustical part of the Rayleigh mode, because the corresponding losses were obscured by the intense diffuse elastic peak [see Fig. 2(b)].

In a recent vibrational study of the Si(111)Al( $\sqrt{3}\times\sqrt{3}$ ) $R30^\circ$  surface, Akavoor *et al.* reported five modes with zone center frequencies of 130, 260, 340, 470, and  $560\text{ cm}^{-1}$ , and little dispersion throughout the SBZ.<sup>10</sup> Since the structures of the Al- and Ga-terminated surfaces are identical, we may compare our results to those of Akavoor *et al.* We note that, while the higher frequencies are rather similar, the two low-frequency modes exhibit an appreciable mass effect, indicating that they may involve large adatom displacements.

### III. THEORY

In order to relate the vibrational spectra to the properties of the Ga-surface bonding we have performed *ab initio* total-energy calculations using the cluster approach. In this approach the surface is replaced by a small cluster which includes only a few surface atoms close to the adsorbate. This approximation is adequate to describe adsorption phenomena determined by localized bonds. Because of the weak dispersion of the measured modes, we expect that the corresponding vibrations are localized, and that they may be reasonably well described by a cluster model. For the total-energy calculations we have used the Kohn-Sham scheme,<sup>11</sup> with the local density approximation for exchange and correlation,<sup>12</sup> and a localized muffin-tin orbital basis,<sup>13</sup> which included *s*, *p*, and *d* functions in all sites. We used an all-electron potential including the core electrons, which have been kept frozen in their atomic configurations. It may be interesting to point out that the Ga 3*d* electrons yielded an appreciable contribution to the surface bond, and had to be included explicitly in the calculation. If one treats the Ga 3*d* electrons as core electrons, the Ga vibration frequency turns out to be too small by about 10%.

In order to study the Ga-surface bond we used the GaSi<sub>14</sub> cluster shown in Fig. 4(a). We relaxed the five degrees of freedom  $u_i$ , defined in Fig. 4(a), and obtained the equilibrium geometry of the cluster by minimizing the total energy. The equilibrium position for the Ga adatom relative to the bulk extrapolated Si(111) surface plane was found to be 1.54 Å, which compares well with the experimental value of 1.49 Å of Zegenhagen *et al.*,<sup>5</sup> obtained with the x-ray standing wave method. In the relaxed geometry atom B was displaced outwards by 0.05 Å, and atom C moved downwards by 0.15 Å with

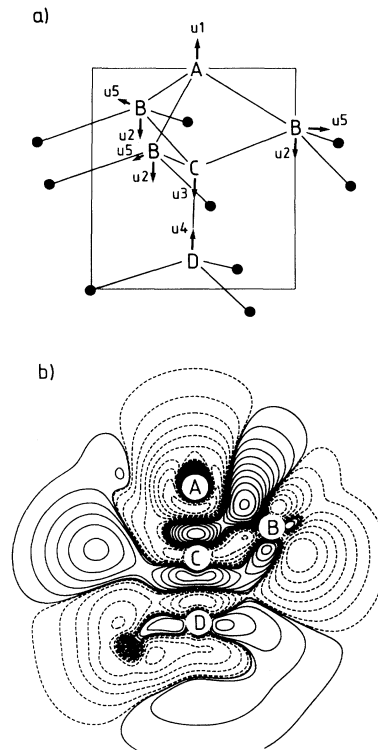


FIG. 4. (a) Si<sub>14</sub>Ga cluster employed to simulate the local environment of a Ga adatom (denoted A) on a Si(111) surface. The remaining atoms are Si. (b) Charge density difference  $\Delta\rho$  on the plane containing atoms A, C, D, and one of type B, indicated by the dashed line in (a). The continuous ( $\Delta\rho > 0$ ) and dashed ( $\Delta\rho < 0$ ) contour lines represent densities given by  $n^2 \times 0.1\text{ e}\text{\AA}^{-3}$ , for  $n = 1, \dots, 10$ .

respect to the bulk positions. The binding energy of the Ga atom, given by  $E = E(\text{GaSi}_{14}) - E(\text{Si}_{14}) - E(\text{Ga})$ , was 3.6 eV.

The electronic charge density difference, given by  $\Delta\rho = \rho(\text{GaSi}_{14}) - \rho(\text{Si}_{14}) - \rho(\text{Ga})$ , and shown in Fig. 4(b), displays the bonding ( $\Delta\rho > 0$ ) and antibonding ( $\Delta\rho < 0$ ) regions of the cluster. Notice the charge depletion on the Ga adatom. This means that as a result of the surface bond a charge transfer from the adatom to the surface took place, reducing the work function of the surface. The induced surface dipole due to one adatom was  $0.27\text{ e}\text{\AA}$ . Notice also the piling up of charge between atoms A and B, and between atoms A and C, indicating direct bonding. As a rough estimate of the bond strength between atoms *I* and *J*, we calculated overlap populations (or bond charges)  $Q_{I,J}$  derived from standard population analysis.<sup>14</sup> For the Ga-Si bonds we found  $Q_{A,B}=0.27\text{ e}$  and  $Q_{A,C}=0.13\text{ e}$ , which are appreciably weaker than  $Q_{I,J} \sim 1.0\text{ e}$ , for the bulk Si-Si bonds. Nevertheless, the nonvanishing bond charge  $Q_{A,C}$  shows that the simple picture of three Ga-Si bonds based on the directed bond model is only partially correct. As a result of the Ga-surface bond, the strength of the B-C bonds is reduced to  $Q_{B,C}=0.60\text{ e}$ , which shows up in Fig. 4(b) as charge depletion between atoms B and C.

TABLE I. Force constant matrix  $k_{ij}$  in atomic units.

$i \setminus j$	1	2	3	4	5
1	0.087	0.022	0.029	-0.001	0.013
2		0.105	-0.041	0.002	0.030
3			0.208	0.115	0.064
4				0.155	0.003
5					0.283

In order to apply the formalism of lattice dynamics we calculated the variation of the total energy as a function of the five degrees of freedom,  $u_i$ . The force constants were obtained by fitting the calculated total energy with the harmonic form

$$V = V_0 + \frac{1}{2} \sum_{i,j} k_{ij} u_i u_j, \quad (1)$$

and are given in Table I in atomic units (1 a.u.= $1.56 \times 10^6$  dyne/cm). The dynamical matrix was calculated according to

$$D_{i,j} = \frac{k_{i,j}}{\sqrt{M_i M_j}}, \quad (2)$$

where  $M_1=M_{\text{Ga}}$ ,  $M_2=M_5=3M_{\text{Si}}$ , and  $M_3=M_4=M_{\text{Si}}$ . The  $5 \times 5$  secular problem yields five frequencies  $\omega_\alpha$  and five eigenvectors  $\vec{\chi}_\alpha = (u_1 \cdots u_5)_\alpha$ . The instantaneous atomic displacements in the  $\alpha$ th normal vibration are given by

$$\vec{u}_\alpha = x_\alpha \vec{\chi}_\alpha, \quad (3)$$

where  $x_\alpha$  is a scalar variable that determines the amplitude of the mode. The normal frequencies and eigenvectors is given in Fig. 5. The displacement pattern of the normal vibrations is indicated by arrows (not drawn to scale).

The highest-frequency mode showing up in our calculations at  $535 \text{ cm}^{-1}$  is the stretching vibration of the  $C$ - $D$  bond, and we assign it to the observed  $550 \text{ cm}^{-1}$  loss. This mode was discussed in detail for the case of the  $\text{Si}(111)\text{Al}(\sqrt{3} \times \sqrt{3})R30^\circ$  surface by Northrup,<sup>15</sup> where the calculated frequency was  $556 \text{ cm}^{-1}$ . The corresponding eigenvector was similar to ours. It had little weight on the adatom, which led Northrup to predict that the frequency of this mode should be almost independent of the mass of the adatom. For a Si adatom adsorbed on  $\text{Si}(111)$ , Daum *et al.*<sup>16</sup> found the same mode at  $575 \text{ cm}^{-1}$ , and pointed out that the reason for the large value of this frequency was the fivefold coordination of atom  $C$ . The motion of atom  $C$  involves the simultaneous stretching of the  $A$ - $C$  bond and contraction of the

$C$ - $D$  bond, giving rise to a larger force constant than in fourfold-coordinated Si, where only one bond stretching occurs. For the case of a Ga adatom, the  $A$ - $C$  bond is weaker than for a Si adatom, but it can be clearly seen in Fig. 4(a).

If the adatom is missing altogether the frequency of the  $C$ - $D$  stretching vibration sinks to  $460 \text{ cm}^{-1}$ . This value has been calculated using a  $\text{Si}_{14}$  cluster identical to that of Fig. 4(a), but without the Ga atom. Therefore we tentatively assign the  $480 \text{ cm}^{-1}$  loss in our experiments to the vertical stretching vibration between Si atoms  $C$  and  $D$  beneath  $T_4$  sites not occupied by Ga adatoms. According to these considerations the splitting of the high-energy vibration of  $\text{Si}(111)$  surfaces into  $480 \text{ cm}^{-1}$  (adsorbate-independent) and higher (adsorbate-dependent) frequencies should be a signature of the  $(\sqrt{3} \times \sqrt{3})$  reconstruction. By contrast,  $(1 \times 1)$  systems show a single (adsorbate-dependent) high-frequency peak. For  $\text{Si}(111)\text{H}(1 \times 1)$ ,<sup>17</sup> and  $\text{Si}(111)\text{As}(1 \times 1)$ ,<sup>18</sup> the high-frequency mode was observed at  $550$  and  $520 \text{ cm}^{-1}$ , respectively.

The  $310 \text{ cm}^{-1}$  mode is the breathing motion of a cluster formed by the Ga atom together with its four neighboring Si atoms of types  $B$  and  $C$ . It includes some stretching of the  $C$ - $D$  bond and possesses an appreciable amplitude in atom  $D$ , which follows the motion of atom  $C$ . We assign this mode to the energy loss measured at  $340 \text{ cm}^{-1}$ . This assignment was already predicted by Akavoor *et al.*, although they find a much larger displacement of the adatom in this mode,<sup>10</sup> probably because of the smaller mass of Al compared with the Ga adatom.

The  $245 \text{ cm}^{-1}$  mode, which involves the stretching of the weak  $A$ - $C$  bond as well as bending forces in the Si double layer, is not seen experimentally. It has a rather small dynamical moment and it may be hidden under the high-energy side of the  $200 \text{ cm}^{-1}$  peak in Fig. 2(a).

The  $194 \text{ cm}^{-1}$  mode, which we assign to the  $200 \text{ cm}^{-1}$  loss of Fig. 2(a), represents the vertical Ga vibration and involves bending and stretching of the three  $A$ - $B$  bonds. This mode was predicted by Northrup for the  $\text{Si}(111)\text{Al}(\sqrt{3} \times \sqrt{3})R30^\circ$  surface, with a frequency of  $266 \text{ cm}^{-1}$ .<sup>15</sup> The difference between the frequencies at the Ga- and Al-terminated surfaces can be explained to a large extent as a mass effect due to the mass difference between the Ga and Al adatoms. However, there are also some differences between the eigenvector for this mode obtained by Northrup, and ours. On the Al-terminated surface the adatom vibrates almost decoupled from the Si substrate, while for the Ga-terminated surface the heavy adatom imposes a substantial displacement on the Si atoms of type  $B$ .

The  $113 \text{ cm}^{-1}$  mode, which we assign to the  $100 \text{ cm}^{-1}$

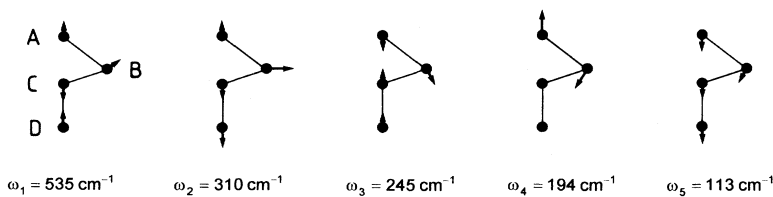


FIG. 5. Schematic representation of the vibrational eigenvectors (arrows not drawn to scale). The frequencies and dynamic dipoles are also given.

loss, involves the collective motion of atoms  $A$ ,  $B$ ,  $C$ , and  $D$  against the bending forces of the surrounding atoms. This motion is similar to that we would expect for an optical surface phonon polarized in the direction perpendicular to the surface. For the Si(111)Al( $\sqrt{3}\times\sqrt{3}$ ) system Akavoor *et al.* ascribed this mode to the back-folded Rayleigh phonon.<sup>10</sup> The corresponding frequency was found  $30\text{ cm}^{-1}$  higher than in the Al-terminated surface, probably due to the mass effect.

#### IV. DISCUSSION

Figure 6 shows the variation of the potential along the normal coordinates related to the modes at  $100$  and  $200\text{ cm}^{-1}$ . The origin of the normal coordinate corresponds to the equilibrium geometry of the cluster. Also indicated in the figure are the energy positions of the ground state and of the first excited states. The harmonic approximation to the potential is indicated by the dashed line. It is apparent that the potentials remain almost symmetric with respect to positive and negative excursions even for large vibration amplitudes. This means that the equilibrium position of the atoms involved in the vibration is not affected by temperature. This result agrees well with the finding of Martinez *et al.* that there was no shift in the mean Ga position as the sample was heated to  $830\text{ K}$ .<sup>6</sup> The vibrational amplitude  $u_{\alpha,n}$  of the  $n$ th excited state of normal mode  $\alpha$  is approximately given by the full width at half maximum of the potential at the excited energy  $\omega_{\alpha,n}$ . At a finite temperature we can estimate the mean square amplitude of the  $\alpha$ th mode by

$$\langle u_{\alpha}^2 \rangle = \frac{\sum_n u_{\alpha,n}^2 e^{-\omega_{\alpha,n}/kT}}{\sum_n e^{-\omega_{\alpha,n}/kT}}. \quad (4)$$

The mean square amplitude of the Ga atom has contributions from the various modes and is given by

$$\langle u_1^2 \rangle = \sum_{\alpha} \chi_{\alpha,1}^2 \langle u_{\alpha}^2 \rangle, \quad (5)$$

where in our case only the  $100\text{ cm}^{-1}$  and  $200\text{ cm}^{-1}$  modes have an appreciable contribution. We have evaluated (5) using the potentials shown in Fig. 6, by summing up the first ten terms of the series in (4). For the vibration amplitude of the Ga atoms, given by  $\langle u_1^2 \rangle^{-1/2}$ , we obtained  $0.11\text{ \AA}$  at  $300\text{ K}$ , and  $0.15\text{ \AA}$  at  $800\text{ K}$ . These values can be compared with those measured by Martinez *et al.*,<sup>6</sup> who found vibrational amplitudes of  $0.10\text{ \AA}$  at  $300\text{ K}$  and  $0.47\text{ \AA}$  at  $830\text{ K}$ . While the room temperature value is in good agreement with our calculations, the high-temperature experimental value is obviously very

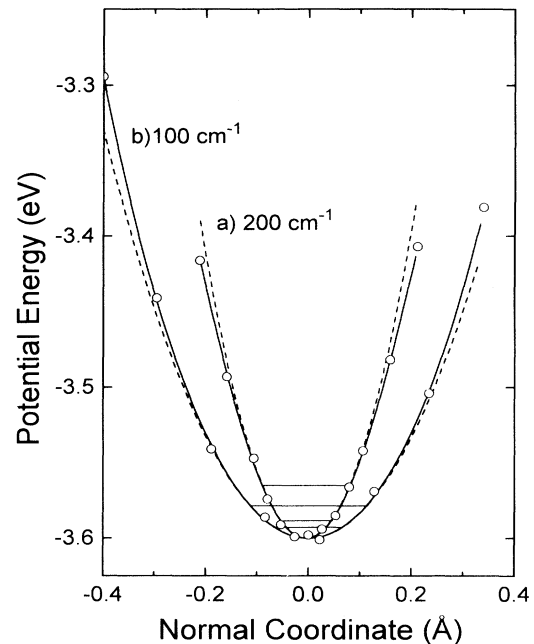


FIG. 6. Variation of the potential along the normal coordinates belonging to the modes at (a)  $200\text{ cm}^{-1}$  and (b)  $100\text{ cm}^{-1}$ . The dashed line represents the harmonic approximation.

large. Furthermore, based on the measured temperature dependence of  $\langle u_1^2 \rangle$  a pronounced decrease of the adatom vibrational frequency of about 15% every  $100\text{ K}$  was predicted. By contrast, in the range between  $40$  and  $300\text{ K}$  we observed no appreciable change of the oscillation frequency. All these discrepancies between our work and that of Martinez *et al.* point to an incomplete treatment of the Si vibrations. These vibrations have a larger amplitude than the vibrations of the comparatively heavy Ga adatom. Actually, a displacement of  $0.47\text{ \AA}$  of the Ga adatoms can be excluded using total-energy considerations. Such an excursion would mean that the distance between the Ga adatom and the Si atom of type  $C$  underneath would be  $2.0\text{ \AA}$ , which is  $0.5\text{ \AA}$  smaller than the sum of the covalent radii of the Si and Ga atoms. According to our total-energy calculations such a large excursion would require an energy of  $1.2\text{ eV}$ , which is very unlikely to be available in the system even at  $800\text{ K}$ .

Summing up, we have performed a detailed study of the vibrations of the Si(111)Ga( $\sqrt{3}\times\sqrt{3}$ ) surface, and we have shown that, while there are no anomalies in the Ga-surface bonding, a simple interpretation of the spectrum in terms of independent Einstein oscillators is inadequate.

<sup>1</sup> J. J. Lander and J. Morrison, Surf. Sci. **2**, 553 (1964).

<sup>2</sup> J. M. Nicholls, B. Reihl, and J. E. Northrup, Phys. Rev. B **35**, 4137 (1987).

<sup>3</sup> A. Kawazu and H. Sakama, Phys. Rev. B **37**, 2704 (1988).

<sup>4</sup> J. Nogami, S. Park, and C. F. Quate, Surf. Sci. **203**, L631 (1988).

<sup>5</sup> J. Zegenhagen, J. R. Patel, P. Freeland, D. M. Chen, J. A. Golovchenko, P. Bedrossian, and J. E. Northrup, Phys.

- Rev. B **39**, 1298 (1988).
- <sup>6</sup> R. E. Martinez, E. Fontes, J. A. Golovchenko, and J. R. Patel, Phys. Rev. Lett. **69**, 1061 (1992).
- <sup>7</sup> R. B. Doak, J. Vac. Sci. Technol. B **7**, 1252 (1989).
- <sup>8</sup> M. Otsuka and T. Ichikawa, Jpn. J. Appl. Phys. **24**, 1103 (1985).
- <sup>9</sup> M. Dayan, Surf. Sci. **149**, L33 (1985).
- <sup>10</sup> P. Akavoor, G. S. Glander, L. L. Kesmodel, and K. Bourke, Phys. Rev. B **48**, 12 063 (1993).
- <sup>11</sup> W. Kohn and L. J. Sham, Phys. Rev. **140**, A1133 (1965).
- <sup>12</sup> S. H. Vosko, L. Wilk, and M. Nussair, Can. J. Phys. **58**, 1200 (1980).
- <sup>13</sup> J. E. Müller, R. O. Jones, and J. Harris, J. Chem. Phys. **79**, 1874 (1982).
- <sup>14</sup> R. S. Mulliken, J. Chem. Phys. **23**, 1833 (1955). For the definition in terms of muffin-tin orbitals, see J. E. Müller, Surf. Sci. **158**, 589 (1986).
- <sup>15</sup> J. E. Northrup, Phys. Rev. Lett. **53**, 683 (1989).
- <sup>16</sup> W. Daum, H. Ibach, and J. E. Müller, Phys. Rev. Lett. **59**, 1593 (1987).
- <sup>17</sup> Ch. Stuhlmann, G. Bogdanyi, and H. Ibach, Phys. Rev. B **45**, 6786 (1992).
- <sup>18</sup> J. Schmidt and H. Ibach, Phys. Rev. B **50**, 14 354 (1994).